https://doi.org/10.15407/ujpe64.7.595

C. VAN HULSE
on behalf of the LHCb Collaboration
University College Dublin
(Belfield, Dublin 4, Ireland; e-mail: cvanhuls@mail.cern.ch)

CENTRAL EXCLUSIVE PRODUCTION AT LHCb

The LHCb collaboration has measured central exclusive production of J/ψ, $\psi(2S)$, and Υ mesons as well as $J/\psi J/\psi$, $J/\psi\psi(2S)$, $\psi(2S)\psi(2S)$, and $\chi_c\chi_c$ meson pairs in proton-proton collisions. The analyses of Υ and charmonium pairs are performed at the centre-of-mass energies of 7 TeV and 8 TeV, and those of J/ψ and $\psi(2S)$ are done at 7 TeV and 13 TeV. The analysis at 13 TeV involves the use of new shower counters. These allow a reduction in the background by vetoing events with activity in an extended region in rapidity. The measurements of central exclusive production at LHCb are sensitive to gluon distributions for Bjorken-x values down to 2×10^{-6} (at 13 TeV). An overview of the LHCb results is presented and compared to existing measurements of other experiments and theoretical calculations.

K e y w o r d s: exclusive photoproduction, ultra-peripheral collisions, generalised parton distributions, parton distribution functions.

1. Introduction

The nucleon structure can be described in three dimensions in terms of the probability to find quarks and gluons as a function of their transverse position inside the nucleon and their longitudinal momentum fraction with respect to the nucleon momentum [1, 2]. The longitudinal direction coincides here with the direction of the probe used to investigate the nucleon. The corresponding probability distributions are called impact-parameter-dependent parton distributions. They are Fourier transforms of generalised parton distributions (GPDs) (see, e.g., Ref. [3]). These GPDs do not have a probabilistic interpretation. Instead, they represent probability amplitudes for a parton with longitudinal momentum fraction $x+\xi$ to be emitted from a nucleon and a parton with longitudinal momentum fraction $x-\xi$ to be absorbed by the nucleon. The nucleon stays intact, but receives a four-momentum transfer squared equal to $-t$. This is represented in Fig. 1, for quarks (left) and gluons (right).

Generalised parton distributions are accessible in exclusive reactions, such as the exclusive production of photons or vector mesons, involving a hard scale. The hard scale is necessary in order to factorise the process into perturbatively calculable parts and non-perturbative parts, which are the GPDs and meson distribution amplitudes in the case of exclusive meson production [4, 5]. Exclusive vector-meson production can be measured in deep-inelastic scattering, as illustrated in Fig. 1, left. The hard scale is provided here by the large virtuality, $Q^2 = -q^2 \gg 1$ GeV^2, of the photon exchanged between the lepton and the nucleon. There exists a multitude of such measurements at fixed-target experiments [6–13] and at lepton-proton colliders, by the H1 and ZEUS collaborations [14–17]. The former series of measurements are mainly sensitive to larger values of Bjorken-x, $x_{\rm B}$, with $\xi \approx x_{\rm B}/(2-x_{\rm B})$, and thus to quark GPDs, while the latter probe lower values of $x_{\rm B}$ down to 10^{-4}, where gluons dominate.

Alternatively, it is possible to use a (quasi-)real photon ($Q^2 \approx 0$ GeV^2) to investigate the nucleon, provided that the particle created in the final state has a large mass component. In the case of exclusive vector-meson production, such as J/ψ or Υ production, the large scale is then provided by the large mass of the meson valence quarks (charm or bottom quarks). The vector mesons originate, as illustrated in Fig. 1, right, from the splitting of the real photon into a quark-antiquark pair ($c\bar{c}$ or $b\bar{b}$). This pair interacts with a nucleon through the exchange of two gluons, and as a result a vector meson is formed in the final state. Quasi-real photopro-

© C. VAN HULSE, 2019

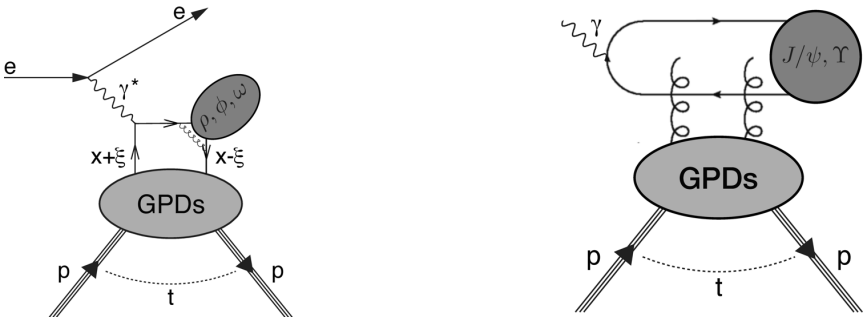

Fig. 1. Diagrams for exclusive production of vector mesons in deep-inelastic scattering (left) and in photoproduction (right). The figure on the left illustrates access to quark GPDs, while the figure on the right shows the diagram for gluon GPDs

duction of vector mesons has been measured in electron-proton collisions by the H1 and ZEUS experiments [16, 18–21]. These measurements probe a photon-nucleon centre-of-mass energy ranging from 30 GeV to 300 GeV.

It is also possible to study photoproduction in ultra-peripheral collisions of protons and ions. In such reactions, the beam particles interact at a large enough distance from each other (in practice more than the sum of their respective nuclear radii) so that they interact through the exchange of colour-neutral objects. The flux of photons emitted by a beam particle is proportional to the square of its atomic charge, and hence photon emission by heavy ions is greater than for protons. There exist measurements of exclusively produced vector mesons in gold-gold collisions by the PHENIX experiment [22], in proton-antiproton collisions by the CDF experiment [23], in lead-lead and proton-lead collisions by the ALICE experiment [24–26] and in proton-proton and lead-lead collisions by the LHCb experiment [27–31]. The covered photon-nucleon centre-of-mass energy ranges from 34 GeV, for the PHENIX experiment, to 1.5 TeV, for the measurements performed by the LHCb collaboration. The very high energy available at the LHC offers the unique possibility to probe the GPDs down to Bjorken-x values of the order of 10^{-6}, i.e., two orders of magnitude lower than for the existing measurements in electron-proton collisions. At such low values of x_{B}, one might also be sensitive to saturation effects [32]. In addition, at such low x_{B}, the exclusive cross section can be approximated in terms of standard gluon parton distribution functions (PDFs) [33–36]. This cross section has a quadratic dependence on the gluon PDFs, and thus provides a higher sensitivity than inclusive measurements, where the dependence is only linear.

2. LHCb Measurements

In central exclusive production of vector mesons in ultra-peripheral collisions, the proton (or ion) emitting the real photon is to a good approximation not altered from its original trajectory, while the proton interacting through the two gluons undergoes a small change in momentum, but remains close to the beam line. The vector meson, in turn, is produced in the central region. At LHCb, this vector meson is generally reconstructed through its decay into a $\mu^+\mu^-$ pair. Hence, the experimental signature for exclusive vector-meson production is two oppositely charged muons in the LHCb detector, with large regions of rapidity, down to close to the beam line, devoid of particle activity. There exists a different process with the same final state, but where the oppositely charged muons originate from the interaction of photons emitted by the respective beam particles. This process is called the Bethe–Heitler process. This production mode of muons forms a continuum background to the exclusive production of vector mesons, and needs to be subtracted from the measured signal. Another source of background is the production of higher-mass vector mesons that decay into the vector meson under study without detection of the other decay products. Furthermore, the production of vector mesons where one or both of the interacting protons dissociate forms another background contribution.

The LHCb detector is a forward detector, covering a rapidity range between 2 and 5. The detector is fully instrumented for particle identification, and is capa-

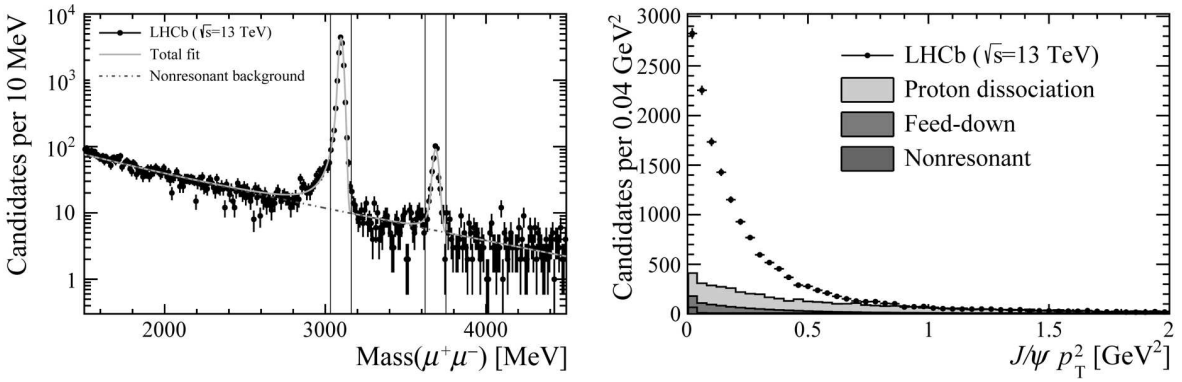

Fig. 2. Dimuon invariant-mass distribution (left) and dimuon squared-transverse-momentum distribution for muon pairs within the J/ψ invariant mass region (right) for data collected at $\sqrt{s} = 13$ TeV, and satisfying the selection requirement imposed by HeRSCheL. Different background contributions are indicated in both figures, while the vertical lines in the figure on the left indicate the selected range in invariant mass for the measurement of J/ψ and $\psi(2S)$

ble of detecting particles with transverse momenta as low as 200 MeV. The LHCb experiment is not instrumented with detectors around the beam line for the detection of protons emerging intact from the interaction or for products from proton dissociation that remain close to the beam line. However, the LHCb experiment is well suited for the measurement of exclusive processes. Firstly, the average number of interactions per beam crossing at the LHCb interaction point ranges only from 1.1 to 1.5, depending on running conditions. Secondly, besides the coverage in rapidity from 2 to 5 by the fully instrumented LHCb detector, the LHCb vertex locator is capable of detecting charged-particle activity for rapidities between –3.5 and –1.5. Also, for Run 2 of the LHC data-taking period (2015–2018), the LHCb experiment was additionally equipped with a series of five stations of scintillators, HeRSCheL [37], placed at –114 m to +114 m from the LHCb interaction point. This allowed for the detection of particle showers in a rapidity range between –10 and –5, and between +5 and +10, and hence for a supplementary reduction of the contribution from background processes.

Measurements of exclusive production of J/ψ and $\psi(2S)$ mesons have been performed by the LHCb experiment using data collected in proton-proton collisions at a centre-of-mass energy $\sqrt{s} = 7$ TeV [28], and part of the data collected at $\sqrt{s} = 13$ TeV [30], amounting to an integrated luminosity of respectively 929 ± 33 pb^{-1} and 204 ± 8 pb^{-1}. This data set allows one to access x_B down to 2×10^{-6}. Both the J/ψ meson and the $\psi(2S)$ meson are reconstructed through

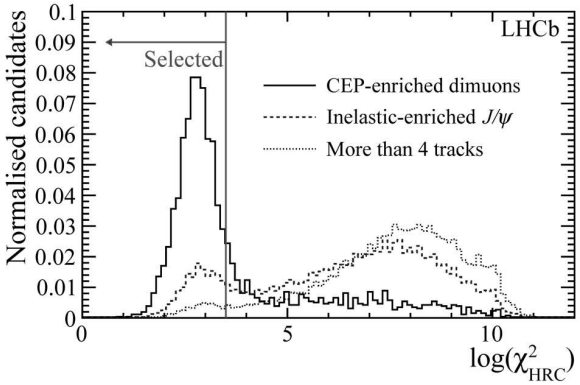

Fig. 3. The distribution, normalised to unit area, of the HeRSCheL discriminating variable χ^2_{HRC}. The continuous, black line corresponds to a sample highly enriched in exclusively produced muon pairs; the blue, dashed line represents the distribution for events enriched in inelastically produced J/ψ mesons, while the purple, short-dashed line contains events with more than four tracks

their decay into muons, which are required to lie in the LHCb detector acceptance, between 2 and 4.5 in rapidity. Furthermore, the transverse momentum squared of the dimuon pair, $p_T^2 \approx -t$, needs to be below 0.8 GeV^2. Finally, the absence of any other detector activity is required.

In Fig. 2, left, the dimuon invariant-mass distribution is shown, while in Fig. 2, right, the squared-transverse-momentum distribution of the muon pair with invariant mass in the J/ψ mass region is presented. The three sources of background contamination to the J/ψ signal are also shown. The back-

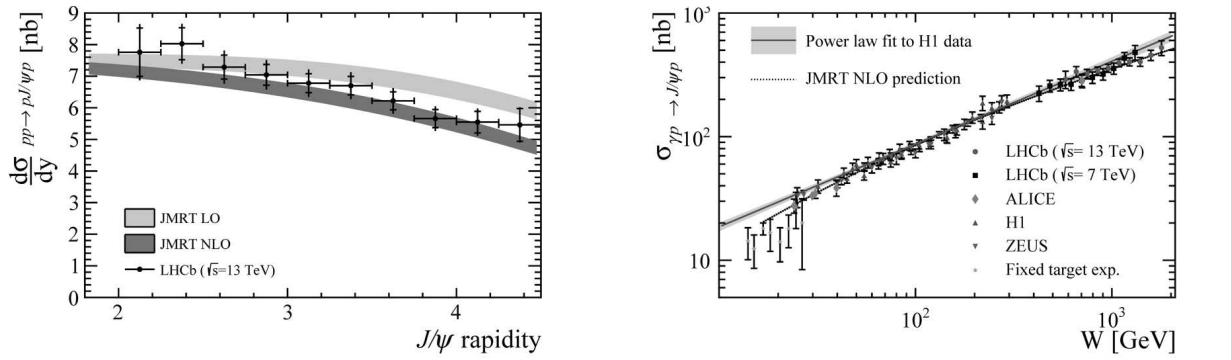

Fig. 4. Cross section differential in rapidity for exclusive J/ψ production (left) and exclusive J/ψ photoproduction cross section as a function of the photon-proton invariant mass (right). The leading-order (yellow band) and next-to-leading-order (green band and dotted line) JMRT calculations [34] are also indicated

ground contribution from the Bethe–Heitler process, labelled nonresonant background, is obtained from a fit to the dimuon mass distribution (see Fig. 2, left). The background from feed-down from exclusive production of $\psi(2S)$ and χ_c mesons is evaluated using $\psi(2S)$ and χ_c signals in experimental data and Monte-Carlo simulation. Finally, the contamination from events where at least one of the protons dissociates is evaluated for Run 1 through a fit of the dimuon transverse-momentum distribution, while for the data collected in Run 2, HeRSCheL has been used. The discriminating power of HeRSCheL is illustrated in Fig. 3. The figure represents distributions of a discriminating variable related to detector activity in HeRSCheL. The continuous, black line is the distribution for a very pure sample of exclusively produced pairs of muons, while the other lines indicate samples enriched in nonexclusive events. From the figure, it is clear that for exclusive events, the discriminating variable is located at low values, whereas for nonexclusive events, the variable extends to higher values. For the selection of exclusive events in Run 2, only events below the value indicated by the red, vertical line are selected. This results in a signal purity of 76% (73%) for J/ψ ($\psi(2S)$). For data collected in Run 1, the signal purity amounts to 62% (52%), where the contribution from proton-dissociative background is about twice as high.

The cross section differential in rapidity for exclusive production of J/ψ in proton-proton collisions at $\sqrt{s} = 13$ TeV is shown in Fig. 4, left. It is seen to decrease at larger values of rapidity. In addition to the experimental data points, theoretical predictions (JMRT) [34], which approximate the cross section in terms of standard gluon PDFs, are shown. There are predictions at leading order in α_S (yellow band) and at next-to-leading order in α_S (green band). The leading-order predictions fail to describe the data at higher rapidities, while the next-to-leading order calculations are in reasonable agreement with the data.

The exclusive vector-meson production cross section in proton-proton collisions is related to the photoproduction cross section through

$$\sigma_{pp\to p\psi p} = r(W_+)k_+\frac{dn}{dk_+}\sigma_{\gamma p\to\psi p}(W_+) + \\ + r(W_-)k_-\frac{dn}{dk_-}\sigma_{\gamma p\to\psi p}(W_-), \quad (1)$$

where r represents the gap survival factor, $k_\pm$ the photon energy, $dn/dk_\pm$ the photon flux, and $W_\pm^2 = 2k_\pm\sqrt{s}$ the photon-proton invariant mass squared. The subscript $+$ $(-)$ corresponds to the situation where the downstream-going (upstream-going) proton is the photon emitter. As can be seen from Eq. (1), the photoproduction cross section appears twice in the expression. The reason resides in the ambiguity on the identity of the proton emitting the real photon. Since the photoproduction cross section corresponding to the low-energy solution W_- only contributes about one third of the time and it has been previously measured and parametrised by the H1 collaboration, this parametrisation is used to fix the low-energy photoproduction cross section, and extract the one at high photon-proton invariant mass. The resulting photoproduction cross section is presented in Fig. 4, right. The data points represented by the red circles are the result at $\sqrt{s} = 13$ TeV,

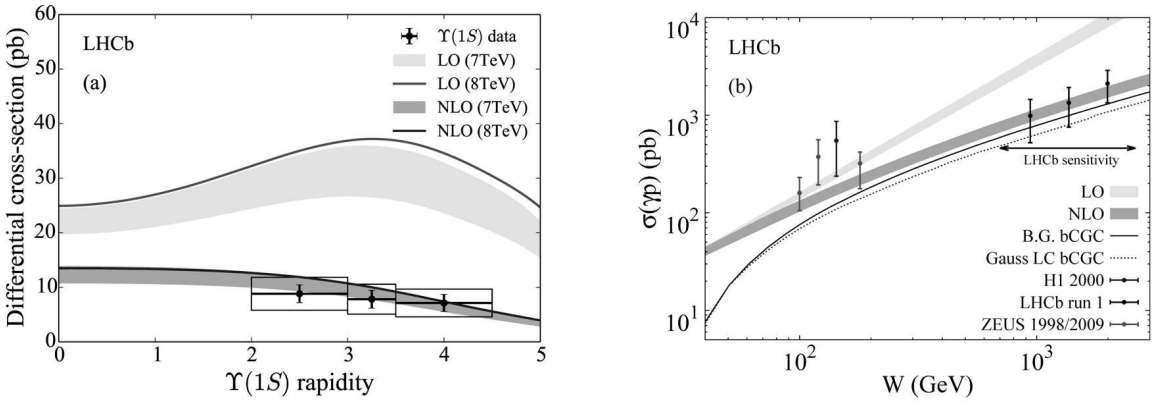

Fig. 5. Cross section differential in rapidity for exclusive $\Upsilon(1S)$ production (left) and exclusive $\Upsilon(1S)$ photoproduction cross section as a function of the photon-proton invariant mass (right). Next-to-leading-order (leading-order) JMRT calculations [34] at $\sqrt{s} = 7$ TeV are indicated by the blue (yellow) band and include uncertainties. The mean value of the next-to-leading-order (leading-order) calculations from JMRT [34] at $\sqrt{s} = 8$ TeV is indicated by the blue (red) line

while those indicated by the black squares are those at $\sqrt{s} = 7$ TeV. Also measurements from the H1 collaboration, from which the parametrisation is taken, the ZEUS and ALICE collaborations as well as from fixed-target experiments [38–40] are presented. The different data sets are in good agreement with each other. The parametrisation from the H1 collaboration is indicated in the figure by the blue band. It is seen to describe the data well at intermediate values of W, but fails at lower and higher values. Also the next-to-leading order JMRT calculations are shown, as indicated by the dotted line. They are in good agreement with the data, describing it well also at low and high values of W. Also for the proton-proton and photoproduction cross section of $\psi(2S)$ (not shown), the next-to-leading order predictions in α_S describe the data well, whereas the leading-order predictions fail to describe the data.

There exist also results from exclusive Υ production by the LHCb collaboration, using data collected in proton-proton collisions in Run 1 at $\sqrt{s} = 7$ TeV and $\sqrt{s} = 8$ TeV, corresponding to a respective luminosity of 0.9 fb^{-1} and 2.0 fb^{-1} [29]. The two data sets are combined in order to increase statistical precision. The data-selection procedure follows that of the measurement for exclusive J/ψ, with a p_T^2 restricted to below 2.0 GeV^2. Given the larger mass of the Υ meson, the lowest values in x_B reach down to 2×10^{-5}. The total proton-proton production cross section for $\Upsilon(1S)$ is determined to be $9.0 \pm 2.1 \pm 1.7$ pb, where the first uncertainty is statistical and the second systematic, while for $\Upsilon(2S)$ it is $1.3 \pm 0.8 \pm 0.3$ pb. For $\Upsilon(3S)$ production, an upper limit on the cross section of 3.4 pb at the 95% confidence level is determined. For the $\Upsilon(1S)$ resonance, the production cross section differential in rapidity and the photoproduction cross section as a function of W are also extracted. They are shown in Fig. 5. Also here, leading-order and next-to-leading order JMRT calculations are presented, and only the next-to-leading order calculations describe the data well. In the figure on the right, also results from the ZEUS and H1 collaborations are shown. These are not able to discriminate between the leading-order and next-to-leading order calculations.

The LHCb collaboration also published results of exclusive production of the charmonium pairs $J/\psi J/\psi$, $J/\psi\psi(2S)$, $\psi(2S)\psi(2S)$, $\chi_{c0}\chi_{c0}$, $\chi_{c1}\chi_{c1}$, and $\chi_{c2}\chi_{c2}$ [41]. These are potentially sensitive to glueballs and tetraquarks. In the framework of describing the exclusive cross section in terms of standard gluon PDFs, they are sensitive to the fourth power of these gluon PDFs. The measurements combine the data collected in proton-proton collisions at $\sqrt{s} = 7$ TeV and $\sqrt{s} = 8$ TeV. The production cross sections are measured to be $\sigma(J/\psi J/\psi) = 58 \pm 10 \pm 6$ pb; $\sigma(J/\psi\psi(2S)) = 63^{+27}_{-18} \pm 10$ pb; $\sigma(\psi(2S)\psi(2S)) < 237$ pb; $\sigma(\chi_{c0}\chi_{c0}) < 69$ nb; $\sigma(\chi_{c1}\chi_{c1}) < 45$ pb; $\sigma(\chi_{c2}\chi_{c2}) < 141$ pb, where only an upper limit is determined for the four last pairs. These results are not corrected for proton dissociation, due to the limited statistical precision. Only for

the production of pairs of $J/\psi J/\psi$ it is possible to estimate the contribution from central exclusive production, which amounts to about 42%, and thus to determine the cross section corrected for proton dissociation, which is 24 ± 9 pb.

3. Summary

Measurements of exclusive production of J/ψ, $\psi(2S)$, and $\Upsilon(nS)$, with $n = 1, 2, 3$, have been performed by the LHCb collaboration. These measurements are sensitive to gluon GPDs and PDFs. The cross sections are measured differentially in rapidity and the photoproduction cross section is extracted as a function of the photon-proton invariant mass. Comparisons to next-to-leading order JMRT calculations show good agreement with these data. Also cross-section measurements of pairs of charmonia have been performed. They are sensitive to the fourth power of the gluon PDFs and potentially to glueballs and tetraquarks. Although not discussed here, there are also preliminary measurements of Bethe-Heitler production in proton-proton collisions [42] and on exclusive χ_c production in proton-proton collisions [42], which is sensitive to the exchange of two gluon pairs. Furthermore there are preliminary results on exclusive production of J/ψ and $\psi(2S)$ in lead-lead collisions [31], which give access to nuclear GPDs and PDFs, and are sensitive to shadowing.

1. M. Burkardt. Impact parameter dependent parton distributions and off-forward parton distributions for $\zeta 0$. *Phys. Rev. D* **62**, 071503 (2000).
2. M. Burkardt. Impact parameter space interpretation for generalized parton distributions. *Int. J. Mod. Phys. A* **18**, 173 (2003).
3. M. Diehl. Generalized parton distributions. *Phys. Rept.* **388**, 41 (2003).
4. J.C. Collins, L. Frankfurt, M.S. Strikman. Factorization for hard exclusive electroproduction of mesons in QCD. *Phys. Rev. D* **56**, 2982 (1997).
5. A.V. Radyushkin. Nonforward parton distributions. *Phys. Rev. D* **56**, 5524 (1997).
6. I. Bedlinskiy *et al.*, [CLAS]. Exclusive η electroproduction at $W > 2$ GeV with CLAS and transversity generalized parton distributions. *Phys. Rev. C* **95**, 035202 (2017).
7. P.E. Bosted *et al.*, [CLAS]. Target and beam-target spin asymmetries in exclusive pion electroproduction for $Q^2 > > 1$ GeV^2. I $ep \to e\pi^+ n$. *Phys. Rev. C* **95**, 035207 (2017).
8. C. Adolph *et al.*, [COMPASS]. Transverse target spin asymmetries in exclusive $\rho 0$ muoproduction. *Phys. Lett. B* **731**, 19 (2014).
9. C. Adolph *et al.*, [COMPASS]. Exclusive ω meson muoproduction on transversely polarised protons *Nucl. Phys. B* **915**, 454 (2017).
10. Fuchey *et al.*, [Jefferson Lab Hall A]. Exclusive neutral pion electroproduction in the deeply virtual regime. *Phys. Rev. C* **83**, 025201 (2011).
11. A. Airapetian *et al.*, [HERMES]. Spin density matrix elements in exclusive ω electroproduction on ^{1}H and ^{2}H targets at 27.5 GeV beam energy. *Eur. Phys. J. C* **74**, 3110 (2014).
12. A. Airapetian *et al.*, [HERMES]. Transverse-target-spin asymmetry in exclusive ω-meson electroproduction. *Eur. Phys. J. C* **75**, 600 (2015).
13. A. Airapetian *et al.*, [HERMES]. Ratios of helicity amplitudes for exclusive ρ^0 electroproduction on transversely polarized protons. *Eur. Phys. J. C* **77**, 378 (2017).
14. F.D. Aaron *et al.*, [H1]. Diffractive electroproduction of ρ and φ mesons at HERA. *JHEP* **05**, 032 (2010).
15. A. Aktas *et al.*, [H1]. Measurement of F-2 (c (c) over-bar) and F-2 (b (b) over-bar) at high Q(2) using the H1 vertex detector at HERA. *Eur. Phys. J. C* **46**, 585 (2006).
16. S. Chekanov *et al.*, [ZEUS]. Exclusive electroproduction of J/ψ mesons at HERA. *Nucl. Phys. B* **695**, 3 (2004).
17. S. Chekanov *et al.*, [ZEUS]. Exclusive ρ^0 production in deep inelastic scattering at HERA. *PMC Phys. A* **1**, 6 (2007).
18. C. Adloff *et al.*, [H1]. Diffractive photoproduction of ψ(2S) mesons at HERA. *Phys. Lett. B* **541**, 251 (2002).
19. A. Aktas *et al.*, [H1]. Elastic J/ψ production at HERA. *Eur. Phys. J. C* **46**, 585 (2006).
20. C. Alexa *et al.*, [H1]. Elastic and proton-dissociative photoproduction of J/ψ mesons at HERA. *Eur. Phys. J. C* **73**, 2466 (2013).
21. S. Chekanov *et al.*, [ZEUS]. Exclusive photoproduction of γ mesons at HERA. *Phys. Lett. B* **680**, 4 (2009).
22. S. Afanasiev *et al.*, [PHENIX]. Photoproduction of J/ψ and of high mass e^+e^- in ultra-peripheral Au + Au collisions at $\sqrt{s_{NN}} = 200$ GeV. *Phys. Lett. B* **679**, 321 (2009).
23. T. Aaltonen *et al.*, [CDF]. Observation of exclusive charmonium production and $\gamma\gamma \to \mu^+\mu^-$ in $p\bar{p}$ collisions at $\sqrt{s} = 1.96$ TeV. *Phys. Rev. Lett.* **102**, 242001 (2009).
24. E. Abbas *et al.*, [ALICE]. Charmonium and e^+e^- pair photoproduction at mid-rapidity in ultra-peripheral Pb–Pb collisions at $\sqrt{s_{NN}} = 2.76$ TeV. *Eur. Phys. J. C* **73**, 2617 (2013).
25. B. Abelev *et al.*, [ALICE]. Coherent J/ψ photoproduction in ultra-peripheral Pb–Pb collisions at $\sqrt{s_{NN}} = 2.76$ TeV. *Phys. Lett. B* **718**, 1273 (2013).
26. B. Abelev *et al.*, [ALICE]. Exclusive J/ψ photoproduction off protons in ultraperipheral p-Pb collisions at $\sqrt{s_{NN}} = = 5.02$ TeV. *Phys. Rev. Lett.* **113**, 232504 (2014).
27. R. Aaij *et al.*, [LHCb]. Exclusive J/ψ and ψ(2S) production in pp collisions at TeV. *J. Phys. G: Nucl. Part. Phys.* **40**, 045001 (2013).

28. R. Aaij *et al.*, [LHCb]. Updated measurements of exclusive J/ψ and $\psi(2S)$ production cross-sections in *pp* collisions at TeV *J. Phys. G: Nucl. Part. Phys.* **41**, 055002 (2014).
29. R. Aaij *et al.*, [LHCb]. Measurement of the exclusive Y production cross-section in *pp* collisions at $\sqrt{s} = 7$ TeV and 8 TeV. *JHEP* **09**, 084 (2015).
30. R. Aaij *et al.*, [LHCb]. Central exclusive production of J/ψ and $\psi(2S)$ mesons in *pp* collisions at $\sqrt{s} = 13$ TeV. *JHEP* **10**, 167 (2018).
31. LHCb Collaboration. Study of coherent J/ψ production in lead-lead collisions at $\sqrt{s_{NN}} = 5$ TeV with the LHCb experiment. CERN-LHCb-CONF-2018-003.
32. N. Armesto *et al.* Exclusive vector meson production at high energies and gluon saturation. *Phys. Rev. D* **90**, 054003 (2014).
33. M.G. Ryskin. Diffractive J/ψ electroproduction in LLA QCD. *Z. Phys. C* **57**, 89 (1993).
34. S.P. Jones *et al.* Probes of the small x gluon via exclusive J/ψ and Y production at HERA and the LHC. *JHEP* **11**, 085 (2013).
35. S.P. Jones *et al.* Exclusive J/ψ process Tamed to probe the low-x gluon. arXiv:1609.09738.
36. C.A. Flett *et al.* Towards a determination of the low x gluon via exclusive J/ψ production. arxiv:1907.06471.
37. K.C. Akiba *et al.* The HeRSCheL detector: High-rapidity shower counters for LHCb. *JINST* **13**, P04017 (2018).
38. M.E. Binkley *et al*, [E104]. J/ψ photoproduction from 60 to 300 GeV/c. *Phys. Rev. Lett.* **48**, 73 (1982).
39. B.H. Denby *et al.*, [E516]. Inelastic and Elastic Photoproduction of $J/\psi(3097)$. *Phys. Rev. Lett.* **52**, 795 (1984).
40. P.L. Frabetti *et al.*, [E687]. A measurement of elastic J/ψ photoproduction cross section at Fermilab E687. *Phys. Lett. B* **316**, 197 (1993).
41. R. Aaij *et al.*, [LHCb]. Observation of charmonium pairs produced exclusively in collisions. *J. Phys. G: Nucl. Part. Phys.* **41**, 115002 (2014).
42. LHCb Collaboration. Central Exclusive Production at LHCb. CERN-LHCb-CONF-2011-022.

Received 08.07.19

Ш. Ван Гулсе
від імені Колаборації LHCb

ЦЕНТРАЛЬНЕ ЕКСКЛЮЗИВНЕ ПРОДУКУВАННЯ НА LHCb

Р е з ю м е

Колаборація LHCb вимірювала центральне ексклюзивне продукування мезонів J/ψ, $\psi(2S)$ і Υ мезонів, а також мезонних пар $J/\psi J/\psi$, $J/\psi\psi(2S)$, $\psi(2S)\psi(2S)$, $\chi_c\chi_c$ в протон-протонних зіткненнях. Аналіз пар мезонів Υ та шармонія виконано при енергіях в системі центра мас 7 та 8 TeB, а для J/ψ та $\psi(2S)$ – при 7 та 13 TeB. В аналізі при 13 TeB були задіяні нові лічильники, які зменшують фон, відсікаючи події з активністю в широкому інтервалі швидкостей. Виміри центрального ексклюзивного продукування на LHCb чутливі до глюонних розподілів для значень бйоркенівської змінної аж до $2 \cdot 10^{-6}$ при 13 TeB. Нами представлено огляд результатів LHCb та їх порівняння з існуючими вимірами в інших експериментах, а також з теоретичними розрахунками.